Journal of Chromatography A, 1441 (2016) 75–82

Contents lists available at ScienceDirect

Journal of Chromatography A

journal homepage: www.elsevier.com/locate/chroma

Characterization of the ultraviolet–visible photoproducts of thiophanate-methyl using high performance liquid chromatography coupled with high resolution tandem mass spectrometry—Detection in grapes and tomatoes

Houda Chayata, Yannick Lassalle, Édith Nicol, Sophia Manolikakes, Yasmine Souissi, Sophie Bourcier, Corinne Gosmini, Stéphane Bouchonnet*

LCM, CNRS, École Polytechnique, Université Paris-Saclay, 91128 Palaiseau, France

ARTICLE INFO

Article history:
Received 13 January 2016
Received in revised form 25 February 2016
Accepted 26 February 2016
Available online 3 March 2016

Keywords:
Thiophanate-methyl
Photolysis
LC-HR-MS/MS
Fruits
Bioassays
Degradation products identification

ABSTRACT

UV–visible irradiation of thiophanate-methyl (TM) led to the formation of nine photoproducts that were characterized by high performance liquid chromatography coupled with high resolution Fourier transform ion cyclotron resonance mass spectrometry (FTICR-MS). Although carbendazime has been reported in the literature to be the major metabolite and photoproduct of thiophanate-methyl, it was not detected in this study. However, an isomer of carbendazime referred as PP2, which was unambiguously characterized owing to CID experiments, was found in great abundance. Grape berries and cherry tomatoes treated with aqueous solutions of thiophanate-methyl were submitted to irradiation under laboratory conditions. TM and PP2 were detected in both peel and flesh of berries. The ability of TM and PP2 to pass through the fruit skin has been shown to be highly compound and matrix dependent. *In vitro* bioassays on *Vibrio fischeri* bacteria showed that the global ecotoxicity of the TM solution increases significantly with the irradiation time. PP2 should likely contribute to this ecotoxicity enhancement since *in silico* estimations for *Daphnia magna* provide a LC50 value seven times lower for PP2 than for the parent molecule.

1. Introduction

Controlling crops pests that can lead to losses in the quality and quantity of farm yields is one of the major aims in modern agriculture. In this context, fungicides are molecules specifically used to prevent or limit the growth of fungal infections. During the preharvest period, these compounds are applied directly on plants and can be subjected to long-term sunlight exposure, leading to their photodegradation [1,2]. Simal Gandara and coworkers have paid particular attention to fungicides analysis in grape, wines and vineyard soils [3–8]. Thiophanate-methyl (dimethyl 4,4′-(*o*-phenylene) bis(3-thioallophanate)) is a commercial systemic fungicide belonging to the family of benzimidazole molecules. It was first introduced to the Japanese market by Nippon Soda Co., in 1970 [9]. This fungicide has a broad spectrum of action and can be used either for its protective or curative activity. Unlike several fungicides belonging to the same family (benomyl, ethyl thiophanate, carbendazim), thiophanate-methyl is still authorized in Europe. Its toxicity was extensively studied in the early 70s, concluding that no significant toxic effect was induced by the molecule [10–12]. However, Saquib et al. reported that thiophanate-methyl induced DNA damage in human lymphocytes [13]. Genotoxic and oxidative properties were also reported in 2014 by Ben Amara et al. in a study devoted to reactive oxygen species production in rat peripheral blood [14]. This molecule is also capable to bind to HSA (Human serum albumin) proteins, leading to molecular conformation changes such as a global decrease in alpha-helices forming these proteins [14,15]. Recent studies have also shown that thiophanate-methyl induces reprotoxic effects; cardone assessed this activity on *Podarcis sicula* and concluded that a long-term exposure to the fungicide leads to the degradation of seminiferous epithelium. An inhibition of the expression of steroid receptors was also observed and may cause infertility [16]. Another study on adult male rabbits revealed that thiophanate-methyl exposure led to a decrease in quantity and quality of sperm cells, a reduction in testosterone levels and histopathologic changes in epididymis [17]. The widespread and intensive use of this molecule for crop protection led to its detection, often above maximum residue limits, in several com-

* Corresponding author.
E-mail address: stephane.bouchonnet@polytechnique.edu (S. Bouchonnet).

http://dx.doi.org/10.1016/j.chroma.2016.02.078
0021-9673/

mercial samples such as rapeseeds, fruits, fruit juices and wines [18–23]. In this context, it must be kept in mind that thiophanate-methyl may undergo biotic and abiotic degradation leading to transformation products for which no toxicological data are available. LC–MS coupling is well known to constitute a technic of choice to determine fungicides in biological matrices [24] but HPLC coupled with sophisticated mass spectrometric methods associating high resolution and tandem mass spectrometry (HR-MS/MS) are often necessary to allow the characterization of metabolites and/or degradation products of emerging pollutants [25–27]. The photochemical behavior of thiophanate-methyl was studied in several matrices. Buchenauer et al. studied the photodegradation rate and mechanism of this molecule in aqueous solutions [28]. The authors reported that approximately 60% of the initial concentration was transformed in 2 days under outdoor environmental conditions, corresponding to a total sunshine duration of 22 h. The main identified photoproduct was methyl benzimidazol-2-yl carbamate (MBC), which is also known to be the main metabolite of thiophanate-methyl. On soil exposed to sunlight, the molecule showed S-oxidation at one of two C=S moieties and also the formation of MBC [29]. Soeda et al. showed that, on glass plates, thiophanate-methyl was rapidly phototransformed *via* the conversion of one C=S function into a ketone one and *via* intramolecular cyclization to from MBC. On grape leaves, apple leaves and bean plants, the major detected photoproduct after an exposition to sunlight was MBC [30,31]. The stability of this metabolite to photolysis was also studied in water and leaves. It was reported to be very stable with less than 10% lost after sunlight exposure for 40 h in aqueous solutions. On leaves of corn plants, no photolysis product were detected after sunlight exposition for 18 h [32].

In this context, the present paper aims to characterize the photoproducts formed during sunlight exposure in water and on fruits, to reassess the phototransformation mechanisms of thiophanate-methyl and to evaluate the impact of photolysis on its environmental toxicity. For that purpose, aqueous solutions were irradiated and analyzed by liquid chromatography coupled with mass spectrometry. The ability of the FT-ICR analyzer to provide ultra-high resolution mass spectra permits direct assignment of exact formulae while its capacity to perform tandem experiments may allow complete structural elucidation through differentiation of isomeric species. CID (Collision Induced Dissociation) experiments were performed on the ESI protonated photoproducts in order to establish their chemical structures. The ability of thiophanate-methyl and its main photoproducts to pass through the fruit peel was investigated on grape and cherry tomato samples. The toxicities of photoproducts were individually estimated *in silico*, with the Toxicity Estimation Software Tool (T.E.S.T.). Finally, the *in vitro* ecotoxicity of the irradiated solution was investigated, for several irradiation times, using *Vibrio fischeri* commercial test kits.

2. Experimental

2.1. Chemicals and reagents

Thiophanate-methyl (99.3% purity) and carbendazime (99.2% purity) were purchased from Sigma– Aldrich (St. Quentin Fallavier, France). Thiophanate-methyl and carbendazime (methyl benzimidazol-2-yl carbamate) will be referred as TM and MBC, respectively; their chemical structures are given in Fig. 1. Thiophanate-methyl-d_6 (hydrogen atoms of both methyl groups are replaced by deuterium atoms, 99.3% purity) was purchased from Cluzeau Info Labo (Courbevoie, France). Methylene chloride, acetonitrile and formic acid were purchased from Sigma Aldrich (chromatographic grade purity: 99.99%).

2.2. Sample preparation

Thiophanate-methyl aqueous solutions at 20 mg L^{-1} (solubility in water: 26.6 mg L^{-1} at 25 °C) were prepared in quartz tubes and sonicated for 10 min. A volume of 60 mL was prepared in each tube, in order to take ten 1 mL samples for kinetic studies without inducing an important change in the surface of solution irradiated (see Section 2.3). For the first part of this study devoted to photolysis in water, the aqueous solutions were irradiated as prepared. The collected samples (100 μL) were extracted by 100 μL methylene chloride for GC–MS analysis. For LC–MS analysis, samples were dried under a gentle nitrogen stream before addition of 100 μL of a H_2O/acetonitrile (90/10 v:v) mixture supplemented with 0.1% formic acid. For the second part of this work, dedicated to UV–visible irradiation on fruits, grape berries and cherry tomatoes were dipped in aqueous solutions of thiophanate-methyl at 5 mg L^{-1} (concentration normally used for crop treatment) for 5 min before being placed in quartz tubes for photolysis experiments. After irradiation, fruit peelings were carefully removed from the flesh using a lancet. Both Peel and pulp samples were separately weighted before being blended using a manual mortar. 1 mL water/acetonitrile 90/10 (v:v) mixture was added to each milling before centrifugation at 12 000 rpm for 90 min at 18 °C. Supernatants were filtered on Acrodisc® glass fiber syringe filters with polytetrafluoroethylene membranes (0.45 μm/13 mm) from Pall Corporation (New York, USA) before LC–HR-MS analysis.

2.3. Photolysis experiments

Photolysis experiments were mostly carried out on a laboratory-made reactor equipped with a high-pressure mercury lamp (HPL-N 125W/542 E27 SC; Phillips, Ivry-sur-Seine, France) delivering radiation at wavelengths ranging from 200 nm to 650 nm. According to manufacturer data, the incident radiation flux was 6200 lm. The reactor consists in six 120 mL quartz tubes disposed in a circle around the lamp and immerged into a sonicator (AL04-12, Advantage-Lab, Switzerland) filled with deionized water. During irradiation, the reactor is regularly cooled by water circulation to avoid uncontrolled heating of the irradiated solutions and to maintain a constant temperature of 40 ± 3 °C. For each experiment, 60 mL of a solution of thiophanate-methyl (see above) were used. To follow the kinetic evolution of photoproducts, a series of experiments was carried out with 10 irradiation times ranging from 0 to 120 min: 0, 10, 20, 30, 40, 50, 60, 80, 100 and 120 min. A constant pH value of 6.0 was measured for each irradiation time. All the irradiated solutions were analyzed by GC–MS and LC–MS. A reference solution of thiophanate-methyl was sonicated and kept 120 min at 40 °C without being submitted to irradiation. Analyses showed that thiophanate-methyl did not undergo any degradation under these conditions. In order to study the phototransformation of TM with a more realistic reproduction of full spectrum sunlight, analogous experiments were performed with a Q-sun test chamber (Xe-1-B/S, Q-Lab Saarbrücken, Germany) equipped with a xenon arc lamp (X-1800, Q-Lab, Saarbrücken, Germany) and a natural light filter (X-7640, Q-Lab, Saarbrücken, Germany). The lamp power was 1800 W and the irradiance 0.5 W/m^2. The photoproducts were the same than those obtained with the high pressure mercury lamp but with a thiophanate-methyl phototransformation rate about 20 times longer (irradiation times up to 40 h were used).

2.4. GC–MS operating conditions

In the present study, GC–MS analysis was conducted for the detection of photoproducts potentially insufficiently polar to be detected in LC–MC coupling. As a result, only the parent molecules and PP2 were detected in GC–MS which means that this method

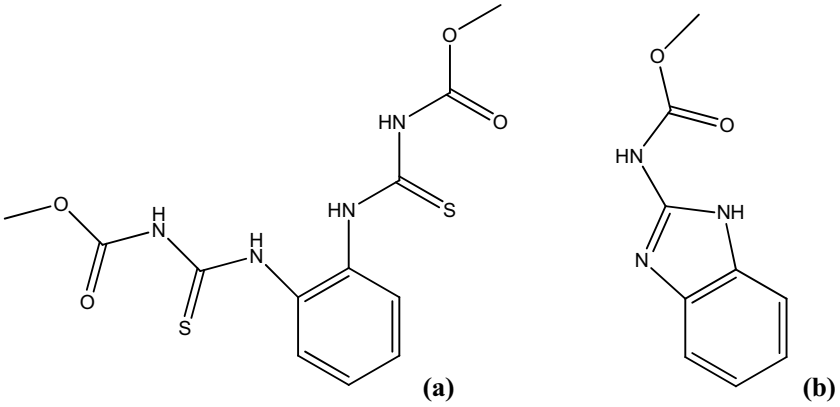

Fig. 1. Chemical structures of thiophanate-methyl (a) and carbendazime (b).

could not be used for the structural elucidation of photoproducts. GC–MS operating conditions are given in the supplementary data file A.

2.5. LC-HR-MS/MS operating conditions

Liquid chromatographic separations were conducted with a liquid chromatography HPLC Alliance 2690 (Waters Technologies, Saint Quentin en Yvelines, France). For all experiments 50 μL of sample were injected and separated on a C_{18} Pursuit-XRsUltra 2.8 μm 502.0 mm column (Agilent Technologies, Les Ulis, France). Elution was performed with a mixture of of solvents A (water, formic acid 0.1%) and B (acetonitrile, formic acid 0.1%) at a flow of 0.2 μL min^{-1}. Percentage of solvent B was increased from an initial value of 10% up to 70% in 20 min and up to 90% after 30 min. The gradient was set at 10% of solvent B for the last 10 min. The HPLC system was coupled with a high resolution mass spectrometer SolarixXR FT-ICR 9.4 Tesla (Bruker Daltonics, Bremen, Germany) for structural elucidation. Ionization was made by an electrospray source in positive mode. A 1:60 split was used between the end of the column and the ESI nebulizer in order to get a flow of 200 μL.h^{-1} in the FT-ICR source. Detection of ions in the FT-ICR was in broadband mode with a 4 Mpt resolution (4.10^6 data points acquired) for a mass range of m/z 57.74–m/z 400 leading to a transient length of 0.8389 s. Capillary was set at −4.5 kV and the end plate offset at −4 kV. Nitrogen was used as nebulizer and drying gas at 1 bar and 4 L min^{-1}, respectively, with a drying gas temperature of 200 °C. Ions were accumulated in the collision cell for 0.5 sec. For MS/MS experiments, the precursor was selected in the quadrupole with an isolation window of 5 Da, collision energy was set from 5 to 20 V. Elementary compositions of parent and fragments ions were determined with the DataAnalysis software using a 3 ppm tolerance.

2.6. In silico *toxicity prediction*

The Toxicity Estimation Software Tool (T.E.S.T.) is an Environmental Protection Agency online available computerized predictive system with Quantitative Structure Activity Relationships (QSAR) mathematical models [33]. T.E.S.T. has a variety of toxicity endpoints used to predict acute toxicity values from the physical properties of the molecular structure. It uses a simple linear function of molecular descriptors such as the octanol–water partition coefficient, steric and/or electronic parameters and also parameters related to the presence/absence of a given chemical group (see Eq. (1)).

$$\text{Toxicity} = ax_1 + bx_2 + c \quad (1)$$

x_1 and x_2 are independent descriptor variables and a, b and c are fitted parameters. Models for assessing toxicity solely from molecular structure are based on information-rich structural descriptors that quantify transport, bulk, and electronic attributes of a chemical structure. Besides molecular weight, the QSAR model employs size-corrected E-values for quantification of molecular bulk. The size-corrected E-values are computed from a rescaled count of valence electrons. Electrotopological state values (E-values) as numerical quantifiers of molecular structure encode information about the electron content (valence, sigma, pi and lone-pair), topology and environment of an atom or a group of atoms in a molecule [34]. The predicted toxicity is estimated by taking an average of the predicted toxicities from the above QSAR methods, provided the predictions are within the respective applicability domains.

2.7. In vitro *ecotoxicity assays*

In vitro tests were carried out using *V. fischeri* commercial test kits. The freeze-dried luminescent bacteria and the luminometer were purchased from Hach Lange (Hach Lange GmbH, Düsseldorf, Germany). The experimental procedure for conducting the bacterial bioluminescence assay is based on the ISO11348-3 protocol (1998) [35]. The analysis was carried out with all dilution and reagents maintained at 15 °C. A working solution of luminescent bacteria was prepared by reconstituting a vial of frozen lyophilized *V. fischeri* cells using 12.5 mL of the reagent diluent provided by the manufacturer. The reconstituted solution was equilibrated for 15 min at 4 °C and the osmolality was adjusted in order to obtain 2% w/v NaCl in each solution or sample. Bacterial reagents were reconstituted just before analysis and the pre-incubation times followed standard protocols. The inhibition percentage (% I) was determined by comparing the relative responses of the control and the diluted sample. Each dilution was tested in duplicate. The sample pH values were approximately 7. A fixed amount of bacteria (100 μl of the reconstituted cell suspension) was added to the dilution vials. Luminescence was measured at time zero (before addition of the test solution) and after 5, 15 and 30 min; it was compared to the value measured for the control solution containing only bacteria.

3. Results and discussion

3.1. Relative amounts and persistency of photoproducts

The relative amounts of thiophanate-methyl and photoproducts were estimated by LC–MS, integrating the chromatographic peaks on the MH^+ ionic current; they are plotted as a function of the irradiation time in Fig. 2. Given that irradiation of TM was performed under laboratory conditions, with a lighting power

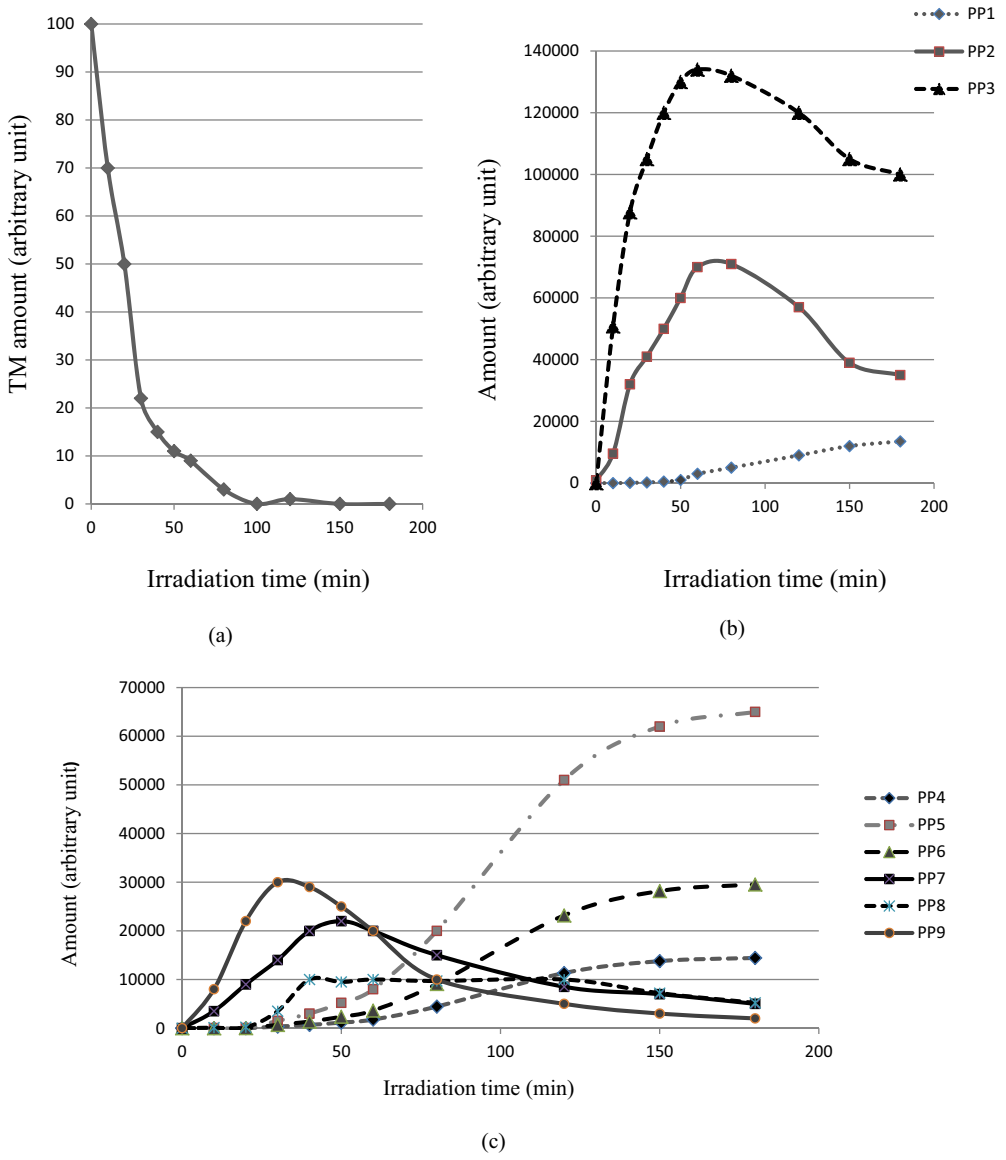

Fig. 2. Relative amounts of thiophanate-methyl and its photoproducts plotted as a function of the irradiation time; (a): thiophanate-methyl, (b): major photoproducts, (c): minor photoproducts.

different from natural solar radiation, these measurements did not aim at determining kinetic constants; they focused on differentiating reaction intermediates from remnant compounds and highlighting the most favorable irradiation time for which all photoproducts are present in order to perform structural elucidation. The concentration of thiophanate-methyl is reduced by half after about 20 min of irradiation; the fungicide is no more detected after 100 min (Fig. 2a). Photoproducts PP1, PP2 and PP3 are globally much more abundant than all others. PP2 and PP3 are detected as soon as irradiation begins; their relative amounts steadily increase to reach a maximum after 50 min of irradiation and decrease until the end of the experiment. They still remain the most abundant photoproducts after 120 min irradiation (Fig. 2b). PP1 is detected after 40 min of irradiation, its amount increases as the concentration of PP2 and PP3 decrease, suggesting that PP1 could result from the photodegradation of PP2 and/or PP3. Photoproducts of higher molecular weights (Fig. 2c) showed lower abundances. PP9 is detected as soon as irradiation begins, PP7 a few minutes later; their relative amounts follow Gaussian function shapes peaking at irradiation times of 30 and 50 min, respectively. Other photoproducts are detected after about 30 min of irradiation and remain in low amounts with the exception of PP5 which displays an increasing abundance until the end of the experiment and thus may be detectable – if present – in "real" samples. A solution irradiated during 80 min was used for the structural elucidation (see Section 3.2).

3.2. Structural elucidation of photoproducts

The fullscan mode chromatogram of the irradiated solution displays ten main peaks: thiophanate-methyl and its nine photoproducts referred as PP1 to PP9, whose relative abundances depend of the irradiation time (see Section 3.1). Table 1 reports the retention time, molecular weight and raw formula of each photoproduct; Table 2 provides the product ions issued from CID experiments. For each photoproduct, the right-hand column of Table 2 gives the number of Deuterium atoms present in each ion when irradiation is performed on TM-d_6. This information is very helpful for structural elucidation; for instance, a shift of +6 atomic mass unit comparing a deuterated photoproduct to its non-deuterated analog

Table 1
Retention times, formulae and chemical structures of thiophanate-methyl photoproducts.

Compound	Retention time (min)	Experimental exact mass of MH^+	Formula	Theoretical exact mass of the neutral	Modification from thiophanate-methyl	Chemical structure
PP1	2.5	134.07137	$C_7H_7N_3$	133.063997	- $C_5H_7NO_4S_2$	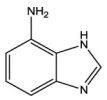
PP2	2.9	192.07692	$C_9H_9N_3O_2$	191.069477	- $C_3H_5NO_2S_2$	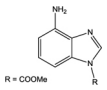
PP3	6.4	277.09359	$C_{12}H_{12}N_4O_4$	276.085855	- H_2S_2	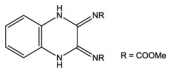
PP4	8.7	327.07613	$C_{12}H_{14}N_4O_5S$	326.068491	- S, + O	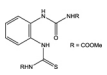
PP5	9.3	325.06043	$C_{12}H_{12}N_4O_5S$	324.052841	- SH_2, + O	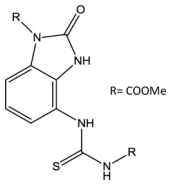
Thiophanate-methyl	10.6	343.05344	$C_{12}H_{14}N_4O_4S_2$	342.045647	–	See Fig. 1
PP6	12.0	325.06043	$C_{12}H_{12}N_4O_5S$	324.052841	- SH_2, + O	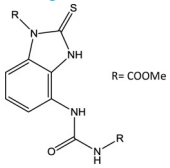
PP7	12.2	307.04984	$C_{12}H_{10}N_4O_4S$	306.042276	- H_4S	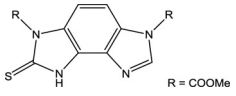
PP8	12.6	339.02198	$C_{12}H_{10}N_4O_4S_2$	338.014347	- H_4	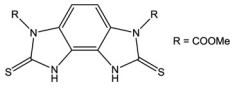
PP9	14.4	341.03768	$C_{12}H_{12}N_4O_4S_2$	340.029997	- H_2	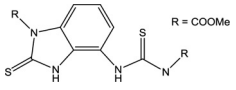

means that the both methyl groups of TM were kept intact during the phototransformation process since no deuterium has been removed. The chemical structures of the photoproducts were postulated on the basis of tandem mass spectrometry experiments and high resolution measurements. The structural elucidation of photoproducts PP3 to PP9 is detailed in the supplementary data file B and the synthesis of dimethyl quinoxaline-2,3-diyldicarbamate – used to establish the chemical structure of PP3 – is described in the supplementary data file C.

The photoproduct PP1 at $M = 133$ has been first assumed to correspond to 2-AB (2-aminobenzimidazole), a currently reported metabolite of MBC (methyl benzimidazol-2-yl carbamate) but CID experiments showed an intense loss of HCN from the protonated molecule, allowing to discard the structure of 2-AB. Fig. 3 shows the easy elimination of HCN from the protonated molecule finally proposed for PP1 (see Table 1). The photoproduct PP2 at $M = 191$ has been first assumed to correspond to MBC but its retention time did not match that of MBC. This is in disagreement with results of previous works that attributed the chemical structure of MBC to the main photoproduct of TM [28,30,31]. Carbendazime has been known for long to be the main metabolite of thiophanate-methyl; that is probably the reason why it has been also considered as its major photoproduct on the basis of molecular mass measurements. Nevertheless, in the present case, MS–MS experiments clearly demonstrate that the structure at $M = 191$ does not match that of MBC. Its chemical structure was proposed on the basis on that of PP1 (please see below) and confirmed by MS/MS experiments.

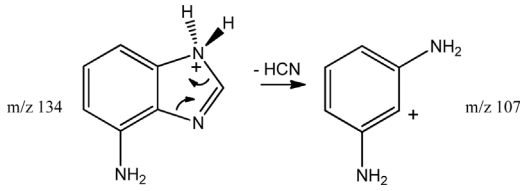

Fig. 3. Elimination of HCN from the pseudomolecular ion of the structure suggested for the photoproduct at $M = 133$.

Table 2
Ions resulting from CID experiments on pseudo molecular ions MH+ of thiophanate-methyl and its main photoproducts.

Compound	MH^+ (in bold) and main product ions	Ion formula	Shift to the theoretical *m/z* [ppm]	Number of D atoms for the deuterated compound
PP1	**134.071143**	$\mathbf{C_7H_8N_3}^+$	1.0	0
	117.044617	$C_7H_5N_2^+$	0.9	0
	107.060288	$C_6H_7N_2^+$	0.8	0
PP2	**192.076572**	$\mathbf{C_9H_{10}N_3O_2}^+$	0.9	3
	160.050412	$C_8H_6N_3O^+$	0.8	0
	135.055188	$C_7H_7N_2O^+$	0.7	0
	132.055535	$C_7H_6N_3^+$	0.7	0
	105.044663	$C_6H_5N_2^+$	0.6	0
PP3	**277.093003**	$\mathbf{C_{12}H_{13}N_4O_4}^+$	0.5	6
	245.066861	$C_{11}H_9N_4O_3^+$	0.2	3
	213.040613	$C_{10}H_5N_4O_2^+$	0.4	0
	201.077043	$C_{10}H_9N_4O^+$	0.2	3
	188.045469	$C_9H_6N_3O_2^+$	−0.1	0
	170.034836	$C_9H_6N_4O^+$	0.3	0
	158.071243	$C_9H_4N_3O^+$	0.2	3
	131.060342	$C_9H_8N_3^+$	0.3	3
PP4	**327.075154**	$\mathbf{C_{12}H_{15}N_4O_5S}^+$	1.9	6
	295.049026	$C_{11}H_{11}N_4O_4S^+$	1.8	3
	252.043341	$C_{10}H_{10}N_3O_3S^+$	1.6	3
	220.017204	$C_9H_6N_3O_2S^+$	1.5	0
	210.087024	$C_9H_{12}N_3O_3^+$	1.4	3
	204.040090	$C_9H_6N_3O_3^+$	1.4	0
	192.076508	$C_9H_{10}N_3O_2^+$	1.3	3
	179.044886	$C_8H_7N_2O_3^+$	1.3	0
	178.060882	$C_8H_8N_3O_2^+$	1.2	0
PP5	**325.059511**	$\mathbf{C_{12}H_{13}N_4O_5S}^+$	1.9	6
	293.033359	$C_{11}H_9N_4O_4S^+$	1.9	3
	261.007246	$C_{10}H_5N_4O_3S^+$	1.7	0
	250.027670	$C_{10}H_8N_3O_3S^+$	1.7	3
PP6	**Idem PP5 + one specific product ion**			
	218.001537	$C_9H_4N_3O_2S^+$	1.5	0
PP7	**307.048993**	$\mathbf{C_{12}H_{11}N_4O_4S}^+$	1.8	6
	275.022846	$C_{11}H_7N_4O_3S^+$	1.8	3
	248.012025	$C_{10}H_6N_3O_3S^+$	1.7	3
	242.996724	$C_{10}H_3N_4O_2S^+$	1.6	0
	217.017519	$C_9H_5N_4OS^+$	1.6	0
	190.006685	$C_8H_4N_3OS^+$	1.4	0
	176.045223	$C_8H_6N_3O_2^+$	1.3	0
PP8	**339.020935**	$\mathbf{C_{12}H_{11}N_4O_4S_2}^+$	2.0	6
	306.994817	$C_{11}H_7N_4O_3S_2^+$	1.9	3
	274.968713	$C_{10}H_3N_4O_2S_2^+$	1.7	0
PP9	**341.036617**	$\mathbf{C_{12}H_{13}N_4O_4S_2}^+$	1.9	6
	309.010491	$C_{11}H_9N_4O_3S_2^+$	1.8	3
	266.004804	$C_{10}H_8N_3O_2S_2^+$	1.7	3
	233.978643	$C_9H_4N_3OS_2^+$	1.7	0
	224.048489	$C_9H_{10}N_3O_2S^+$	1.5	3
	192.022334	$C_8H_6N_3OS^+$	1.4	0

3.3. Irradiation on grape berries and cherry tomatoes

As real field samples were not available for this study, three grape berries and three cherry tomatoes were dipped in 5 mg L^{-1} aqueous solutions of thiophanate-methyl for 5 min before being irradiated during 80 min. Peelings and flesh were then manually separated, weighted and milled. A 1 mL water/acetonitrile 90/10 (v:v) mixture was added to each milling before centrifugation and filtration, as described in the experimental section, before being analysed by LC-HR-MS. TM-d_6 was added at 5 mg L^{-1} in the analysed solution as an internal standard. The chromatographic peaks of TM, TM-d_6 and photoproducts were integrated on the MH^+ ion current of each species. The corresponding concentrations were estimated from that of TM-d_6 using the peak areas determined and a simple rule of three. Considering that the response factors of TM and its photoproducts may be significantly different, the results given in Table 3 may only constitute rough evaluations; they are based on the exact weights of peelings and pulps collected for each sample and are thus expressed in mg kg^{-1}. Each result corresponds to a mean value determined from the 3 grape samples or from the 3 tomato samples (CV < 20%).

Table 3
Estimated concentrations (mg kg^{-1}) for thiophanate-methyl and photoproducts PP2 and PP4 determined in the peel and flesh of grape berries and cherry tomatoes (mean values for 3 samples in each case, CV < 20%).

Grape berries					Cherry tomatoes			
Peel			Pulp		Peel		Pulp	
TM	PP2	PP4	TM	PP2	TM	PP2	TM	PP2
3.9	0.9	0.9	0.9	0.9	0.9	0.9	0.9	0.1

As shown in Table 3, only thiophanate-methyl and PP2 were detected in all media, *i.e.* grape skin, grape flesh, tomato peel and tomato flesh; PP4 was detected only in grape peel and the other photoproducts previously determined were not detected. Detecting or not detecting a photoproduct cannot be correlated to its abundance in aqueous solution: PP3 is not detected in any media while it is the major product formed in solution, whatever the irradiation time. In the same way, the presence or not of dissolved oxygen in the aqueous solution to form hydroxyl radicals under UV irradiation does not constitute a criterion for photoproduct detection. One might have thought that oxidized compounds would not be detected because of the quick vaporisation of water from the

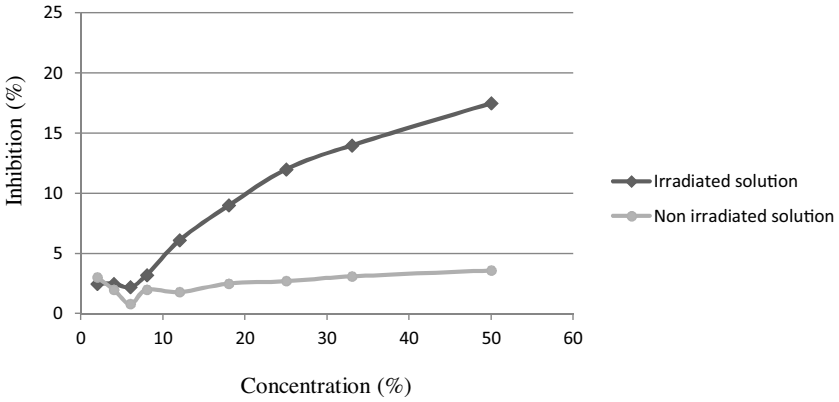

Fig. 4. Response–dose curves plotted from the results of the *Vibrio fischeri* bioluminescence inhibition test after 30 min incubation.

"treating" solution but the presence of PP4 – in which a sulfur atom has been replaced by an oxygen one – in grape skin indicates that oxidation is quick enough to occur before water vaporization (according to the pathway suggested in additional content B) or that it may involve atmospheric O_2. In any case, the results on fruits demonstrate very strong matrix effects on the phototransformation processes.

TM and PP2 can pass through the peel of both fruits; the ratios [concentration in pulp/concentration in peel] are 0.2 in grape *vs* 1.0 in cherry tomato for TM and 1.0 in grape *vs* 0.1 in cherry tomato for PP2. These results show that the peel permeability strongly depends on the product and the fruit considered. It is of concern because it means that water rinsing of the fruit before consumption, which is generally the only cleaning process in both domestic and industrial uses, is not sufficient to remove these contaminants. As an example, a chromatogram of a grape flesh extract is displayed in the supplementary data file D.

3.4. In silico *estimated toxicities*

In order to evaluate the toxicity of thiophanate-methyl and the photoproducts detected in grape and cherry tomato, *i.e.* PP2 and PP4, the toxicity simulation *in silico* tool described above was used. We chose in this study to report only the most significant results, *i.e. Daphnia magna* LD50 and oral rat LD50 toxicities, as well as developmental toxicity (the later including endocrine perturbation and reprotoxicity). These results, displayed in the supplementary data file E, show that thiophanate-methyl, PP2 and PP4 represent a potential risk for development. Thiophanate-methyl has been reported to induce endocrine perturbation and to reduce the fertility of rabbits through reduction of the number and quality of spermatozoa [36]. According to other studies, carbendazime, whose chemical structure is close to that of PP2, can induce tumors as well as aberrant sexual differentiations [37]. Both fungicides act as endocrine disruptors at very low amounts [38]. The *in silico* estimations also show that PP4 may induce a developmental toxicity slightly higher than thiophanate-methyl (a 1.04 value was determined for PP4 against 0.98 for the parent molecule). To date, there is no available literature data explaining the toxicity of this kind of structure. Oral rat LD50 values of 1764.7 and 1523.8 mg/kg were estimated for thiophanate-methyl and PP2, respectively. These values correspond to a low toxicity according to the Hodge and Sterner classification (LD50 ranging from 500 to 5000 mg/kg) [39], they are in good agreement with results of previous studies [40]. *In silico* tests showed that PP4 with a LD50 estimated at 371.2 mg/kg might be significantly more toxic than thiophanate-methyl. The reduction of the LD50 value seems to be related to the number of cycles in the chemical structure of the photoproduct but this hypothesis has to be confirmed. PP2 also induces a higher toxicity than the parent molecule for *D. magna* with LC50 values of 0.76 mg/L and 5.37 mg/L, respectively. No LC50 value was estimated for PP4 since the T.E.S.T. program had no sufficient parameters for the corresponding structure.

3.5. *Ecotoxicity assays on* V. fischeri *bacteria*

Fig. 4 (left hand) displays the inhibition percentage after 30 min of incubation of a non-irradiated thiophanate-methyl solution (20 mg/L) and of the same solution irradiated for 80 min. The comparison of both curves shows that the irradiated solution is significantly more toxic than the reference one. For instance, at 10% (v:v), the irradiated solution induces a inhibition percentage six times higher than the reference one. These preliminary results show that some photoproducts are more toxic than the parent molecule, in agreement with *in silico* estimations. Fractionation of the photolyzed solution followed by *in vitro* tests on each fraction should permit to determine the photoproduct(s) mainly responsible for this increase in toxicity.

4. Conclusions

UV–visible irradiation of thiophanate-methyl led to the formation of nine photoproducts that were characterized by LC-HR-MS/MS. As a consequence of the high number of degrees of freedom of TM as well as its numerous π bonds and lone pairs of electrons, all the photoproducts but one result from cyclization mechanisms involving the aromatic ring and one of the side chains or both of them. As usually seen in photochemistry, oxidation processes were also observed, most of the time accompanied by the elimination of one or two sulphur atoms. Although it has been reported in the literature to be the major metabolite and photoproduct of thiophanate-methyl, carbendazime was not detected in this study. An isomer of MBC, unambiguously characterized with CID experiments was found in great abundance. It suggests that the compound assumed to correspond to MBC on the basis of molecular mass measurements in previous studies could be actually the one characterized in this work (PP2). This study illustrates how the combination of high resolution with CID experiments may permit the unambiguous structural elucidation of degradation products. If FT-ICR-mass spectrometers provide the best resolution and mass accuracy, such characterization studies may also be achieved using Q-TOF (Quadrupole-Time-Of-Flight) or orbitrap mass analyzers. Grape berries and cherry tomatoes treated with 5 mg L^{-1} aqueous solutions of thiophanate-methyl were submitted to irradiation under laboratory conditions. TM and PP2 were detected in both peel and flesh of berries. The ability of TM and PP2 to pass through the

fruit skin is strongly compound and matrix dependent: higher for PP2 in grape and higher for TM in cherry tomato. *In vitro* assays on *V. fischeri* bacteria showed that the global ecotoxicity of the TM solution significantly increases with irradiation time. PP2 should likely contribute to this ecotoxicity enhancement since *in silico* estimations for *D. magna* provide a LC50 value seven times lower for PP2 than for the parent molecule. Given that no real samples – sunlight irradiated under field conditions – were available for this study, one must be cautious interpreting the above results. Nevertheless, the potential toxicity of the main photoproduct and its ability to pass through fruit peel suggest paying particular attention to fruits treated with thiophanate-methyl and submitted to intense and/or long sunshine exposure.

Acknowledgments

Financial supports from the National FT-ICR network (FR 3624CNRS) and from the *Ile de France Région* for conducting the research are gratefully acknowledged.

Appendix A. Supplementary data

Supplementary data associated with this article can be found, in the online version, at http://dx.doi.org/10.1016/j.chroma.2016.02.078.

References

[1] H.D. Burrows, L.M. Canle, J.A. Santaballa, S. Steenken, Reaction pathways and mechanisms of photodegradation of pesticides, J. Photochem. Photobiol. B 67 (2) (2002) 71–108.
[2] T. Katagi, Photodegradation of pesticides on plant and soil surfaces, Rev. Environ. Contam. T. 182 (2004) 1–189.
[3] R.M. Gonzalez-Rodriguez, R. Rial-Otero, B. Cancho-Grande, J. Simal-Gandara, Determination of 23 pesticide residues in leafy vegetables using gas chromatography-ion trap mass spectrometry and analyte protectants, J. Chromatogr. A 1196 (2008) 100–109.
[4] R. Rial-Otero, B. Cancho-Grande, J. Simal-Gandara, Multiresidue method for fourteen fungicides in white grapes by liquid–liquid and solid-phase extraction followed by liquid chromatography-diode array detection, J. Chromatogr. A 992 (2003) 121–131.
[5] C.F. Gonzalez, R. Rial-Otero, B.C. Grande, J.S. Gandara, Determination of fungicide residues in white grapes for winemaking by gas chromatography with mass spectrometric detection and assessment of matrix effects, J. AOAC Int. 86 (2003) 1008–1014.
[6] R. Rial-Otero, R.M. Gonzalez-Rodriguez, B. Cancho-Grande, J. Simal-Gandara, Parameters affecting extraction of selected fungicides from vineyard soils, J. Agric. Food Chem. 52 (2004) 7227–7234.
[7] E. Pose-Juan, B. Cancho-Grande, R. Rial-Otero, J. Simal-Gandara, The dissipation rates of cyprodinil, fludioxonil, procymidone and vinclozoline during storage of grape juice, Food Control 17 (2006) 1012–1017.
[8] R.M. Gonzalez-Rodriguez, R. Noguerol-Pato, C. Gonzalez-Barreiro, B. Cancho-Grande, J. Simal-Gandara, Application of new fungicides under good agricultural practices and their effects on the volatile profile of white wines, Food Res. Int. 44 (2001) 397–403.
[9] V. Morton, T. Staub, A Short History of Fungicides, 2015 (accessed 08-2015) http://www.apsnet.org/publications/apsnetfeatures/Pages/Fungicides.aspx.
[10] Y. Hashimoto, T. Makita, N. Ohnuma, T. Noguchi, Acute toxicity on dimethyl 4,4′-*o*-phenylene bis (3-thioallophanate), thiophanate-methyl fungicide, Toxicol. Appl. Pharmacol. 23 (4) (1972) 606–615.
[11] T. Makita, Y. Hashimoto, T. Noguchi, Mutagenic, cytogenetic and teratogenic studies on thiophanate-methyl, Toxicol. Appl. Pharmacol. 24 (2) (1973) 206–215.
[12] J.A. Thomas, L. Schein, Effects of thiophanate and thiophanate-methyl on the male reproductive system of the mouse, Toxicol. Appl. Pharmacol. 30 (1) (1974) 129–133.
[13] Q. Saquib, A.A. Al-Khedhairy, S. Al-Arifi, A. Dhawan, J. Musarrat, Assessment of methyl thiophanate–Cu(II) induced DNA damage in human lymphocytes, Toxicol. In Vitro 23 (5) (2009) 848–854.
[14] I. Ben Amara, H. Ben Saad, B. Cherif, A. Elwej, S. Lassoued, C. Kallel, N. Zeghal, Methyl-thiophanate increases reactive oxygen species production and induces genotoxicity in rat peripheral blood, Toxicol. Mech. Methods 24 (9) (2014) 679–687.
[15] J. Li, X. Liu, C. Ren, J. Li, F. Sheng, Z. Hu, In vitro study on the interaction between thiophanate methyl and human serum albumin, J. Photochem. Photobiol. B 94 (3) (2009) 158–163.
[16] A. Cardone, Testicular toxicity of methyl thiophanate in the Italian wall lizard (*Podarcis sicula*): morphological and molecular evaluation, Ecotoxicology 21 (2) (2012) 512–523.
[17] F. Bououza, L. Mallem, M. Boulakoud, Evaluation of methyl thiophanate toxicity on fertility and histology of testis and epidydim in male rabbit, Adv. Environ. Biol. 8 (5) (2014) 1196–1204.
[18] E. Dreassi, A. Zanfini, A.T. Zizzari, C. La Rosa, M. Botta, G. Corbini, LC/ESI/MS/MS determination of postharvest fungicide residues in citrus juices, Lwt-Food Sci. Technol. 43 (9) (2010) 1301–1306.
[19] A. Economou, H. Botitsi, S. Antoniou, D. Tsipi, Determination of multi-class pesticides in wines by solid-phase extraction and liquid chromatography-tandem mass spectrometry, J. Chromatogr. A 1216 (31) (2009) 5856–5867.
[20] X.M. Fu, L.J. Zhang, R.L. Wu, J.D. Wang, Simultaneous determination of thiabendazole thiophanate methyl and iprodione in muskmelons by liquid chromatography–mass spectrometry, Chin. J. Anal. Chem. 32 (8) (2004) 1047–1049.
[21] A.R. Fernandez-Alba, A. Tejedor, A. Aguera, M. Contreras, J. Garrido, Determination of imidacloprid and benzimidazole residues in fruits and vegetables by liquid chromatography–mass spectrometry after ethyl acetate multiresidue extraction, J. AOAC Int. 83 (3) (2000) 748–755.
[22] H.Y. Chen, W. Zhang, Z.H. Yang, M.M. Tang, J. Zhang, H.J. Zhu, P. Lu, D.Y. Hu, K.K. Zhang, Determination of thiophanate-methyl and carbendazim in rapeseed by solid phase extraction and ultra-high performance chromatography with photodiode array detection, Instrum. Sci. Technol. 43 (5) (2015) 511–523.
[23] A. Sannino, Investigation into contamination of processed fruit products by carbendazim, methyl thiophanate and thiabendazole, Food Chem. 52 (1) (1995) 57–61.
[24] C. Soler, J. Mañes, Y. Picó, Comparison of liquid chromatography using triple quadrupole and quadrupole ion trap mass analyzers to determine pesticide residues in oranges, J. Chromatogr. A 1067 (1–2) (2005) 115–125.
[25] Y. Picó, D. Barceló, Transformation products of emerging contaminants in the environment and high-resolution mass spectrometry: a new horizon, Anal. Bioanal. Chem. 407 (21) (2015) 6257–6273.
[26] M. Farré, Y. Picó, D. Barceló, Application of ultra-high pressure liquid chromatography linear ion-trap orbitrap to qualitative and quantitative assessment of pesticide residues, J. Chromatogr. A 1328 (2014) 66–79.
[27] E.M. Thurman, I. Ferrer, A.R. Fernández-Alba, Matching unknown empirical formulas to chemical structure using LC/MS TOF accurate mass and database searching: example of unknown pesticides on tomato skins, J. Chromatogr. A 1067 (1) (2005) 127–134.
[28] H. Buchenauer, L.V. Edgington, F. Grossmann, Photochemical transformation of thiophanate-methyl and thiophanate to alkyl benzimidazol-2-yl carbamates, Pestic. Sci. 4 (3) (1973) 343–348.
[29] United States Environmental Protection Agency Reregistration eligibility decision on thiophanate-methyl, 2015 (accessed 08-2015) http://www.epa.gov/oppsrrd1/reregistration/REDs/tm_red.pdf.
[30] Y. Soeda, S. Kosaka, T. Noguchi, Identification of alkyl 2-benzimidazolecarbamates as a major metabolite of thiophanates fungicide in/on the bean plant, Agric. Biol. Chem. 36 (5) (1972) 817–823.
[31] Y. Soeda, S. Kosaka, T. Noguchi, The fate of thiophanate-methyl fungicide and its metabolites on plant leaves and glass plates, Agric. Biol. Chem. 36 (6) (1972) 931–936.
[32] J.R. Fleeker, H.M. Lacy, Photolysis of methyl 2-benzimidazolecarbamate, J. Agric. Food. Chem. 25 (1) (1977) 51–55.
[33] Toxicity Estimation Software Tool (TEST).
[34] L.H. Hall, B. Mohney, L.B. Kier, The electrotopological state: structure information at the atomic level for molecular graphs, J. Chem. Inf. Comput. Sci. 31 (1991) 76–82.
[35] ISO, Water quality, in: Freshwater Algal Growth Inhibition Test with Unicellular Green Algae, International Organisation for Standardisation, Switzeland, 1998, pp. 11348–11353.
[36] F. Bououza, L. Mallem, M. Boulakoud, Evaluation of methyl thiophanate toxicity on fertility and histology of testis and epidydim in male rabbit, Adv. Environ. Biol. 8 (5) (2014) 1196–1204.
[37] H. Morinaga, T. Yanase, M. Nomura, T. Okabe, K. Goto, N. Harada, H. Nawata, A benzimidazole fungicide, benomyl, and its metabolite, carbendazim, induce aromatase activity in a human ovarian granulose-like tumor cell line (KGN), Endocrinology 145 (4) (2004) 1860–1869.
[38] F. Maranghi, C. Macrı, C. Ricciardi, A.V. Stazi, M. Rescia, A. Mantovani, Histological and histomorphometric alterations in thyroid and adrenals of CD rat pups exposed in utero to methyl thiophanate, Reprod. Toxicol. 17 (5) (2003) 617–623.
[39] E. Schlede, E. Genschow, H. Spielmann, G. Stropp, D. Kayser, Oral acute toxic class method: a successful alternative to the oral LD50 test, Regul. Toxicol. Pharm. 42 (2004) 15–23.
[40] W.J. Hayes Jr., E.R. Laws Jr., Handbook of Pesticide Toxicology. Classes of Pesticides, vol. 3, Academic Press Inc., New York, NY, 1991, pp. 1457.